



M.Bellanger

on behalf of the participants:

CNAM: M.Bellanger, D.LeRuyet, D.Roviras, M.Terré

TUM: J.Nossek, L.Baltar, Q.Bai, D.Waldhauser

TUT: M.Renfors, T.Ihalainen, A.Viholainen, T.H.Stitz

UCL: J.Louveaux, A.Ikhlef

SINTEF: V.Ringset, H.Rustad

CTTC: M.Najar, C.Bader, M.Payaro

RA-CTI: D. Katselis, E. Kofidis, L. Merakos, A. Merentitis, N. Passas,

A. Rontogiannis, S. Theodoridis, D. Triantafyllopoulou, D. Tsolkas, D. Xenakis

UNINA: M.Tanda, T.Fusco

CEA-LETI: M.Huchard

AGILENT : J.Vandermot

ALCATEL-LUCENT/UK : A.Kuzminskiy

ALCATEL-LUCENT/DE : F.Schaich

COMSIS : P.Leclair, A.Zhao

## **FBMC physical layer : a primer**

### **Summary:**

The filter bank multicarrier (FBMC) transmission technique leads to an enhanced physical layer for conventional communication networks and it is an enabling technology for the new concepts and, particularly, cognitive radio.

The objective of this document is to provide an overview of FBMC, with emphasis on the features which impact communication networks. The only prerequisite for reading the document is basic knowledge in digital signal processing, in particular sampling theory, fast Fourier transform (FFT) and finite impulse response (FIR) filtering. More thorough developments on the techniques described, as well as alternative and more sophisticated methods, are available on the website <http://www.ict-phydyas.org>.

The presentation begins with the direct application of the FFT to multicarrier communications, pointing out the limitations of this simplistic approach, and, particularly, the spectrum leakage. Then, it is shown that the FFT approach can evolve to a filter bank approach which is straightforward to design and implement. For each block of data, the time window is extended beyond the multicarrier symbol period and the symbols overlap in the time domain. This time overlapping is at the basis of conventional efficient single carrier modems where interference between the symbols is avoided if the channel filter satisfies the Nyquist criterion. This fundamental principle is readily applicable to multicarrier transmission. Regarding implementation, the filter bank approach is just an extension of the direct FFT approach and it can be realized with an extended FFT. An alternative scheme,

requiring less computations, is the so-called polyphase network (PPN)-FFT technique, which keeps the size of the FFT but adds a set of digital filters.

Contrary to OFDM (orthogonal frequency division multiplexing) where orthogonality must be ensured for all the carriers, FBMC requires orthogonality for the neighbouring sub-channels only. In fact, OFDM exploits a given frequency bandwidth with a number of carriers, while FBMC divides the transmission channel associated with this given bandwidth into a number of sub-channels. In order to fully exploit the channel bandwidth, the modulation in the sub-channels must adapt to the neighbour orthogonality constraint and offset quadrature amplitude modulation (OQAM) is used to that purpose. The combination of filter banks with OQAM modulation leads to the maximum bit rate, without the need for a guard time or cyclic prefix as in OFDM.

The effects of the transmission channel are compensated at the sub-channel level. The sub-channel equalizer can cope with carrier frequency offset, timing offset and phase and amplitude distortions, so that asynchronous users can be accommodated. When FBMC is employed in burst transmission, the length of the burst is extended to allow for initial and final transitions due to the filter impulse response. These transitions may be shortened if some temporary frequency leakage is allowed, for example whenever a frequency gap is present between neighbouring users. As a multicarrier scheme, FBMC can benefit from multiantenna systems and MIMO techniques can be applied. Due to OQAM modulation, adaptations are necessary for some MIMO approaches, in the diversity context.

FBMC systems are likely to coexist with OFDM systems. Since FBMC is an evolution of OFDM, some compatibility can be expected. In fact, the initialization phase can be common to both and efficient dual mode implementation can be realized.

In the multiuser context, the sub-channels or groups of sub-channels allocated to the users are spectrally separated as soon as an empty sub-channel is present in-between. Therefore, users do not need to be synchronized before they gain access to the transmission system. This is a crucial facility for uplink in base station ruled networks or for future opportunistic communications. In cognitive radio, the FBMC technique offers the possibility to carry out the functions of spectrum sensing and transmission with the same device, jointly and simultaneously. Moreover, the users enjoy a guaranteed level of spectral protection.

**Contents:**

## Summary

- 1) The FFT as a multicarrier modulator
- 2) Filtering effect of the FFT
- 3) Prototype filter design - Nyquist criterion
- 4) Extending the FFT to implement the filter bank
- 5) PPN-FFT to reduce computational complexity
- 6) OQAM modulation
- 7) Effects of the transmission channel
- 8) Sub-channel equalization
- 9) Burst transmission with FBMC
- 10) MIMO-FBMC
- 11) Compatibility with OFDM
- 12) FBMC in networks

Phydyas website

## 1. The FFT as a multicarrier modulator

The inverse fast Fourier transform (iFFT) can serve as a multicarrier modulator and the fast Fourier transform (FFT) can serve as a multicarrier demodulator. A multicarrier transmission system is obtained and the transmitter and the receiver are shown in Fig.1.

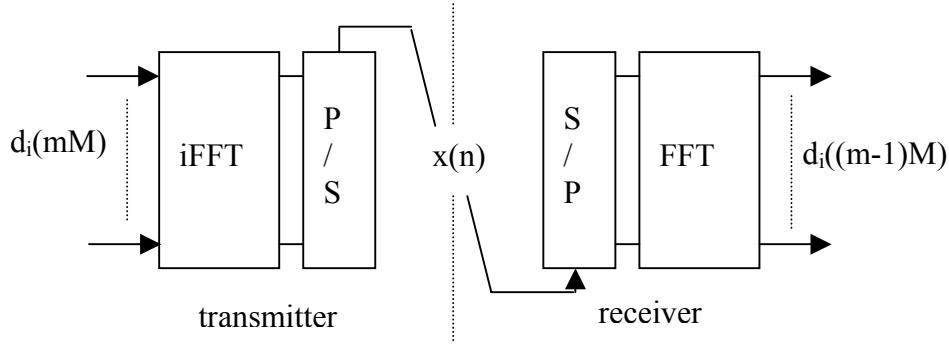


Fig.1. Multicarrier modulation with the FFT

It is obvious from the figure that the block of data at the input of the iFFT in the transmitter is recovered at the output of the FFT in the receiver, since the FFT and the iFFT are cascaded.

The detailed description of the operations is as follows.

The size of the iFFT and the FFT is  $M$  and a set of  $M$  data samples,  $d_i(mM)$  with  $0 \leq i \leq M-1$ , is fed to the iFFT input. For  $mM \leq n < (m+1)M$  the iFFT output is expressed by

$$x(n) = \sum_{i=0}^{M-1} d_i(mM) e^{j2\pi \frac{i(n-mM)}{M}}$$

The set of  $M$  samples so obtained is called a multicarrier symbol and  $m$  is the symbol index. For transmission in the channel, a parallel-to-serial (P/S) converter is introduced at the output of the iFFT and the samples  $x(n)$  appear in serial form. The sampling frequency of the transmitted signal is unity, there are  $M$  carriers and the carrier frequency spacing is  $1/M$ . The duration of a multicarrier symbol  $T$  is the inverse of the carrier spacing,  $T=M$ . Note that  $T$  is also the multicarrier symbol period, which reflects the fact that successive multicarrier symbols do not overlap in the time domain.

An illustration is given in Fig.2 for  $i=2$  and  $d_2(mM) = \pm 1$ . The transmitted signal  $x(n)$  is a sine wave and the duration  $T$  contains  $i=2$  periods. Similarly,  $d_i(mM)$  is transmitted by  $i$  periods of a sine wave in the duration  $T$ . Overall, the transmitted signal is a collection of sine waves such that the symbol duration contains an integer number of periods. In fact, it is the condition for data recovery, the so-called orthogonality condition.

At the receive side, a serial-to-parallel (S/P) converter is introduced at the input of the FFT. The data samples are recovered by

$$d_i(mM) = \frac{1}{M} \sum_{n=mM}^{mM+M-1} x(n) e^{-j2\pi \frac{i(n-mM)}{M}}$$

Note also in Fig.1 that, due to the cascade of P/S and S/P converters, there is a delay of one multicarrier symbol at the FFT output with respect to the iFFT input.

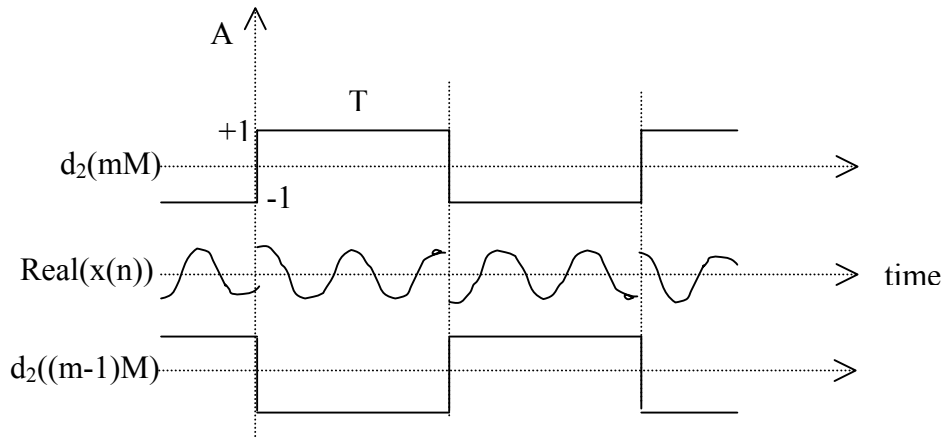


Fig.2. Data and transmitted signals

For the proper functioning of the system, the receiver (FFT) must be perfectly aligned in time with the transmitter (iFFT). Now, in the presence of a channel with multipath propagation, due to the channel impulse response, the multicarrier symbols overlap at the receiver input and it is no more possible to demodulate with just the FFT, because intersymbol interference has been introduced and the orthogonality property of the carriers has been lost.

Then, there are 2 options:

- 1) extend the symbol duration by a guard time exceeding the length of the channel impulse response and still demodulate with the same FFT. The scheme is called OFDM.
- 2) keep the timing and the symbol duration as they are, but add some processing to the FFT. The scheme is called FBMC, because this additional processing and the FFT together constitute a bank of filters.

The present document is concerned with this second approach and, as an introduction, it will first be shown that the FFT itself is a filter bank.

## 2. Filtering effect of the FFT

Let us assume that the FFT is running at the rate of the serially transmitted samples. Considering Fig.1, the relationship between the input of the FFT and the output with index  $k = 0$  is the following

$$y_0(n) = \frac{1}{M} [x(n-M) + \dots + x(n-1)] = \frac{1}{M} \sum_{i=1}^M x(n-i)$$

This is the equation of a low-pass linear phase FIR filter with the  $M$  coefficients equal to  $1/M$ . Disregarding the constant delay, the frequency response is

$$I(f) = \frac{\sin \pi f M}{M \sin \pi f}$$

It is shown in Fig.3, where the unit on the frequency axis is  $1/M$ .

In the same conditions, the FFT output with index  $k$  is expressed by

$$y_k(n) = \frac{1}{M} \sum_{i=0}^{M-1} x(n-M+i) e^{-j2\pi ki/M}$$

Changing variables and replacing  $i$  by  $M - i$ , an alternative expression is

$$y_k(n) = \frac{1}{M} \sum_{i=1}^M x(n-i) e^{j2\pi ki/M}$$

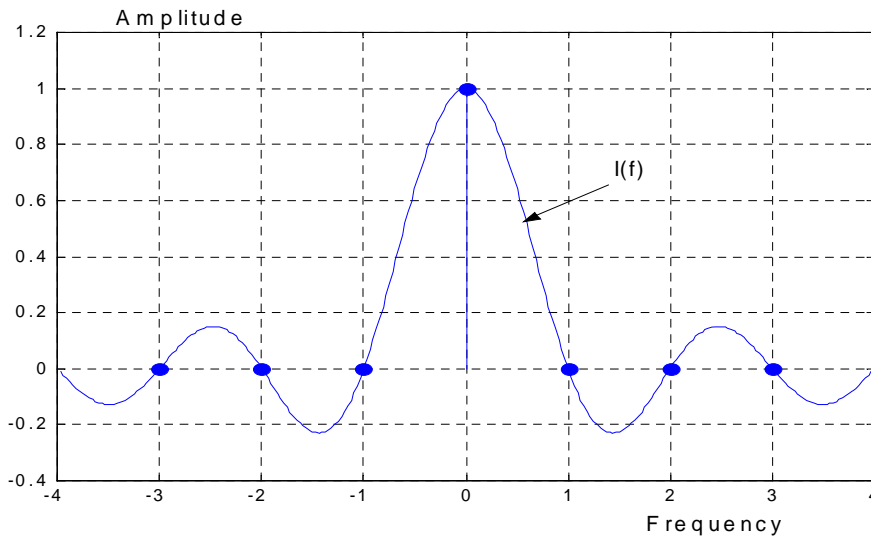


Fig.3. FFT filter frequency response and coefficients in the frequency domain

The filter coefficients are multiplied by  $e^{j2\pi ki/M}$ , which corresponds to a shift in frequency by  $k/M$  of the frequency response. When all the FFT outputs are considered, a bank of  $M$  filters is obtained, as shown in Fig.4, in which the unit on the frequency axis is  $1/M$ , the sub-carrier spacing. The orthogonality condition appears through the zero crossings: at the frequencies which are integer multiples of  $1/M$ , only one filter frequency response is non-zero.

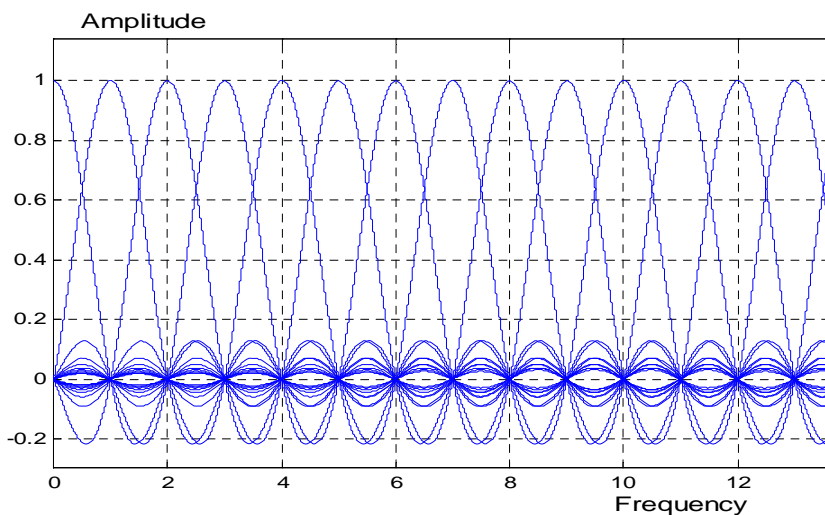


Fig.4. The FFT filter bank (frequency unit: sub-carrier spacing)

An FIR filter can be defined by coefficients in the time domain or by coefficients in the frequency domain. The two sets of coefficients are equivalent and related by the discrete Fourier transform (DFT). Returning to the first filter in the bank, the DFT of its impulse response consists of a single pulse, as shown in Fig.3. In fact, the frequency coefficients are

the samples of the frequency response  $I(f)$ , which, according to the sampling theory, is derived from them through the interpolation formula.

In the terminology of filter banks, the first filter in the bank, the filter associated with the zero frequency carrier, is called the prototype filter, because the other filters are deduced from it through frequency shifts. It is clearly apparent in Fig.4 that  $I(f)$  is the frequency response of a prototype filter with limited performance, particularly out-of-band attenuation. In order to reduce the out-of-band ripples, it is necessary to increase the number of coefficients in the time domain and, equivalently, in the frequency domain. Then, in the time domain, the filter impulse response length exceeds the multicarrier symbol period  $T$ . In the frequency domain, additional coefficients are inserted between the existing coefficients, allowing for a better control of the filter frequency response.

Prototype filters are characterised by the overlapping factor  $K$ , which is the ratio of the filter impulse response duration  $\Theta$  to the multicarrier symbol period  $T$ . The factor  $K$  is also the number of multicarrier symbols which overlap in the time domain. Generally,  $K$  is an integer number and, in the frequency domain, it is the number of frequency coefficients which are introduced between the FFT filter coefficients.

Now, the question is how to design the prototype filter and transmit data in such a manner that no intersymbol interference occurs, in spite of the overlapping.

### 3. Prototype filter design – Nyquist criterion

Digital transmission is based on the Nyquist theory: the impulse response of the transmission filter must cross the zero axis at all the integer multiples of the symbol period. The condition translates in the frequency domain by the symmetry condition about the cut-off frequency, which is half the symbol rate. Then, a straightforward method to design a Nyquist filter is to consider the frequency coefficients and impose the symmetry condition.

In transmission systems, the global Nyquist filter is generally split into two parts, a half-Nyquist filter in the transmitter and a half-Nyquist filter in the receiver. Then, the symmetry condition is satisfied by the squares of the frequency coefficients. The frequency coefficients of the half-Nyquist filter obtained for  $K=2,3$  and 4 are given in Table1.

K	$H_0$	$H_1$	$H_2$	$H_3$	$\sigma^2$ (dB)
2	1	$\sqrt{2}/2$	-	-	-35
3	1	0.911438	0.411438	-	-44
4	1	0.971960	$\sqrt{2}/2$	0.235147	-65

Table 1. Frequency domain prototype filter coefficients

In the frequency domain, the filter response consists of  $2K-1$  pulses, as shown in Fig.5 for  $K=4$ . The continuous frequency response, also shown in Fig.5, is obtained from the frequency coefficients through the interpolation formula for sampled signals which yields

$$H(f) = \sum_{k=-(K-1)}^{K-1} H_k \frac{\sin(\pi(f - \frac{k}{MK})MK)}{MK \sin(\pi(f - \frac{k}{MK}))}$$

The out-of-band ripples have nearly disappeared and a highly selective filter has been obtained.

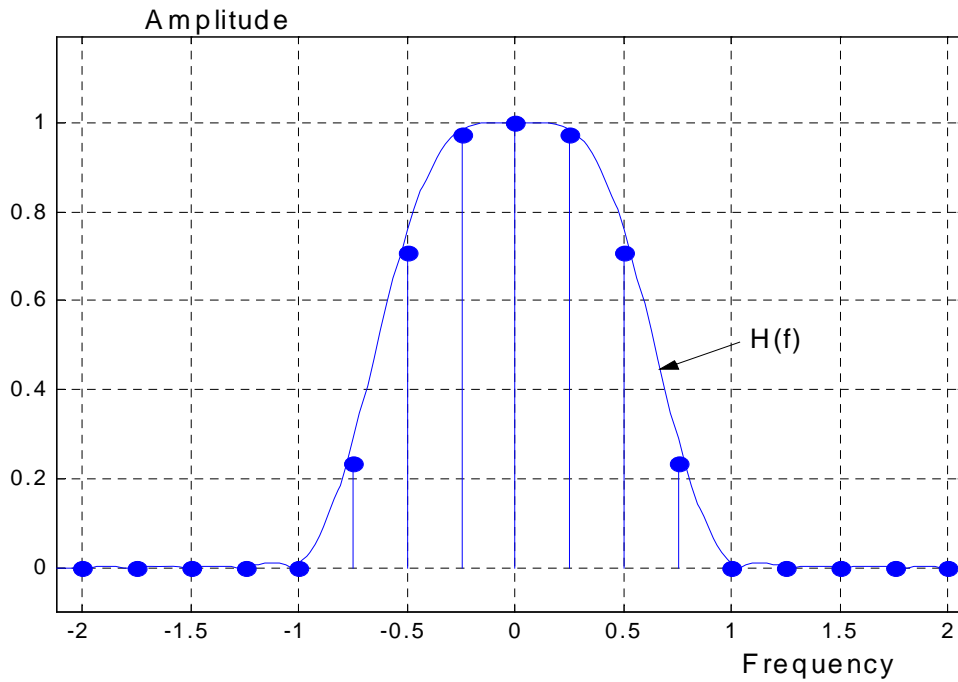


Fig.5. Prototype filter frequency coefficients and frequency response for K=4.

The impulse response  $h(t)$  of the filter is given by the inverse Fourier transform of the pulse frequency response, which is

$$h(t) = 1 + 2 \sum_{k=1}^{K-1} H_k \cos(2\pi \frac{kt}{KT})$$

It is shown in fig.6 for the filter length L=1024, the number of sub-channels M=256 and K=4.

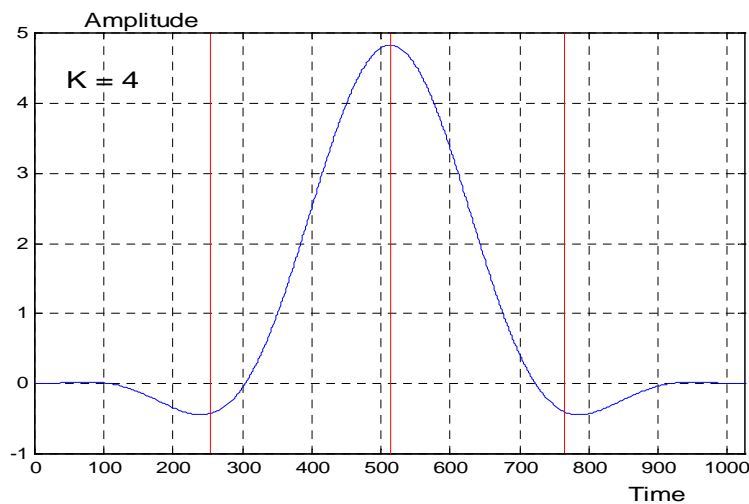


Fig.6. Impulse response of the prototype filter for overlapping factor K=4.

Once the prototype filter has been designed, the filter bank is obtained by the frequency shifts  $k/M$ , as in the FFT case. The filter with index  $k$  is obtained by multiplying the prototype filter coefficients by  $e^{j2\pi ki/M}$ , as mentioned in section 2 for the FFT. A section of the filter bank derived in that manner is shown in Fig.7. The sub-channel index corresponds to the

frequency axis and the sub-carrier spacing is unity. A key observation is that the sub-channels with even index (odd index) do not overlap. This has a great impact on systems as will be emphasized below. In fact, a particular sub-channel overlaps in frequency with its neighbours only.

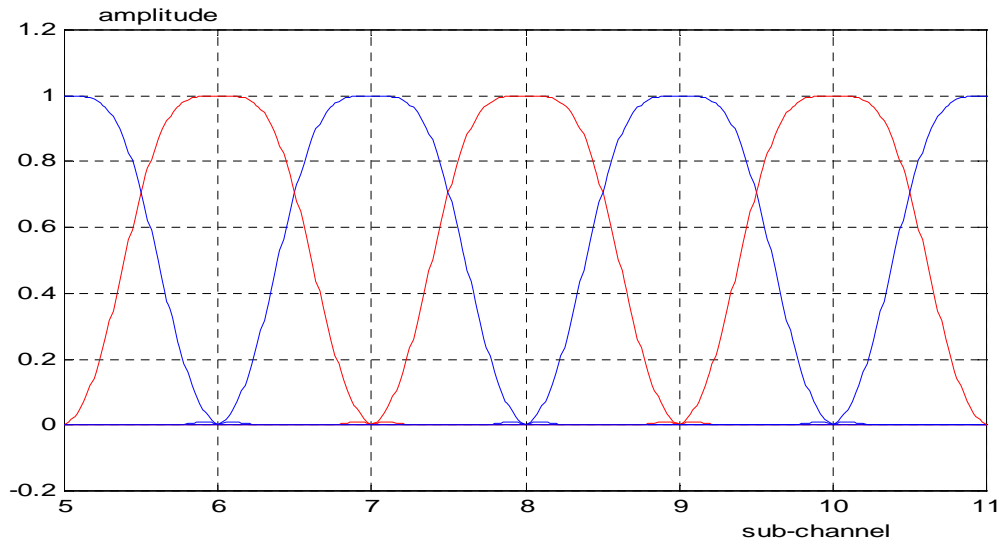


Fig.7. Section of a filter bank based on the prototype with  $K=4$

The intersub-channel interference frequency response is important because it determines the modulation scheme.

As illustrated in Fig.7, for a given sub-channel, the receiver filter of this sub-channel overlaps with the transmitter filter of the neighbouring sub-channel. Considering the frequency coefficients of two neighbouring sub-channels, the overlap concerns  $K-1$  coefficients and the frequency coefficients of the interference filter are

$$G_k = H_k H_{K-k} \quad ; \quad k = 1, \dots, K-1$$

The set of coefficients is symmetrical and for  $K = 4$

$$G_1 = 0.228553 = G_3 \quad ; \quad G_2 = 0.5$$

As previously mentioned, the interference frequency response is derived with the help of the interpolation formula which yields

$$G(f) = \sum_{k=1}^3 G_k \frac{\sin(\pi(f - \frac{k}{MK})MK)}{MK \sin(\pi(f - \frac{k}{MK}))}$$

The frequency response of the interference filter is shown in Fig.8 for  $K = 4$ . In the time domain, the interference filter impulse response is given by the inverse Fourier transform

$$g(t) = [ G_2 + 2G_1 \cos(2\pi \frac{t}{KT}) ] e^{j2\pi \frac{t}{2T}}$$

This is a crucial result, which determines the type of modulation which must be used to dodge interference. The factor  $e^{j2\pi \frac{t}{2T}} = \cos(\pi/T) + j\sin(\pi/T)$  reflects the symmetry of the frequency coefficients and, due to this factor, the imaginary part of  $g(t)$  crosses the zero axis at the integer multiples of the symbol period  $T$  while the real part crosses the zero axis at the odd multiples of  $T/2$ . The zero crossings are interleaved and it is the basis for the OQAM modulation presented in a later section.

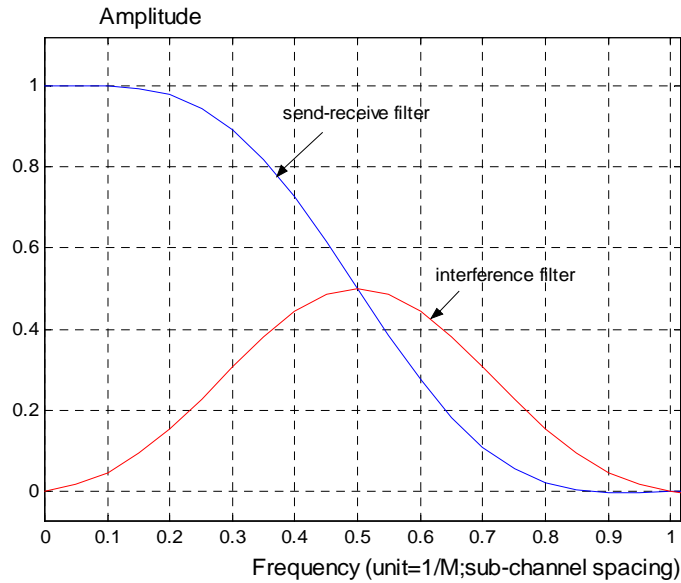


Fig.8. Frequency responses of the sub-channel filter and interference filter

Now, considering the complete system, the frequency coefficients of the transmitter-receiver filter are the squares of those of the prototype. The corresponding responses are given by

$$h_2(t) = 1 + 2 \sum_{k=1}^{K-1} H_k^2 \cos(2\pi \frac{kt}{KT})$$

and

$$H_2(f) = \sum_{k=-(K-1)}^{K-1} H_k^2 \frac{\sin(\pi(f - \frac{k}{MK})MK)}{MK \sin(\pi(f - \frac{k}{MK}))}$$

This is a Nyquist filter and its frequency response is shown in Fig.8 for  $K = 4$ .

An important parameter related to the prototype filter design is the “background noise” power. Actually, it is the residual interference power due to the non-orthogonality of the carriers beyond the neighbouring sub-channels. It is measured, for example, by loading all the sub-channels but one with uncorrelated unit power signals and measuring the signal power in the unloaded sub-channel. The values  $\sigma^2$  obtained for different overlapping factors  $K$  are reported in the last column of Table 1. The parameter is important for system design because it impacts bit loading and spectrum sensing.

Once a design is available comes the implementation.

#### 4. Extending the FFT to implement the filter bank

The simple scheme depicted in Fig.1 can be adapted to implement the filter bank, it is just sufficient to extend the iFFT and the FFT.

In section 1, a data element is applied to one input of the iFFT and it modulates one carrier. In a filter bank with overlapping factor  $K$ , as shown in Fig.5, a data element modulates  $2K-1$  carriers. Thus, the filter bank in the transmitter can be implemented as follows

- an iFFT of size  $KM$  is used, to generate all the necessary carriers,
- a particular data element  $d_i(mM)$ , after multiplication by the filter frequency coefficients, is fed to the  $2K-1$  inputs of the iFFT with indices  $(i-1)K+1, \dots, (i+1)K-1$ . Practically, the data element is spread over several iFFT inputs and the operation can be called “weighted frequency spreading”.

For each set of input data, the output of the iFFT is a block of  $KM$  samples and, since the symbol rate is  $1/M$ ,  $K$  consecutive iFFT outputs overlap in the time domain. Therefore, the filter bank output is provided by an overlap and sum operation, as shown in Fig.9.

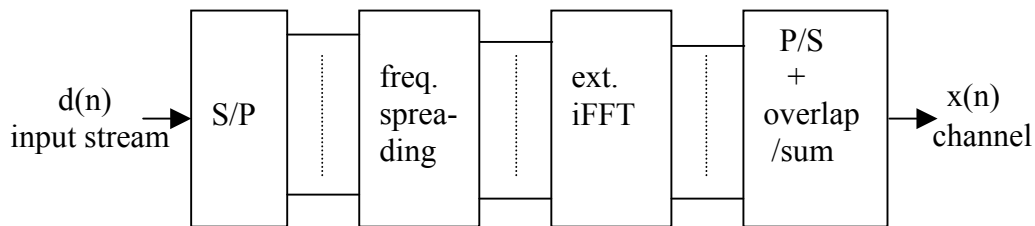


Fig.9. Principle of the filter bank based transmitter implemented with iFFT extension

Details of the implementation are given in Fig.10 for the overlapping factor  $K = 4$ . The figure

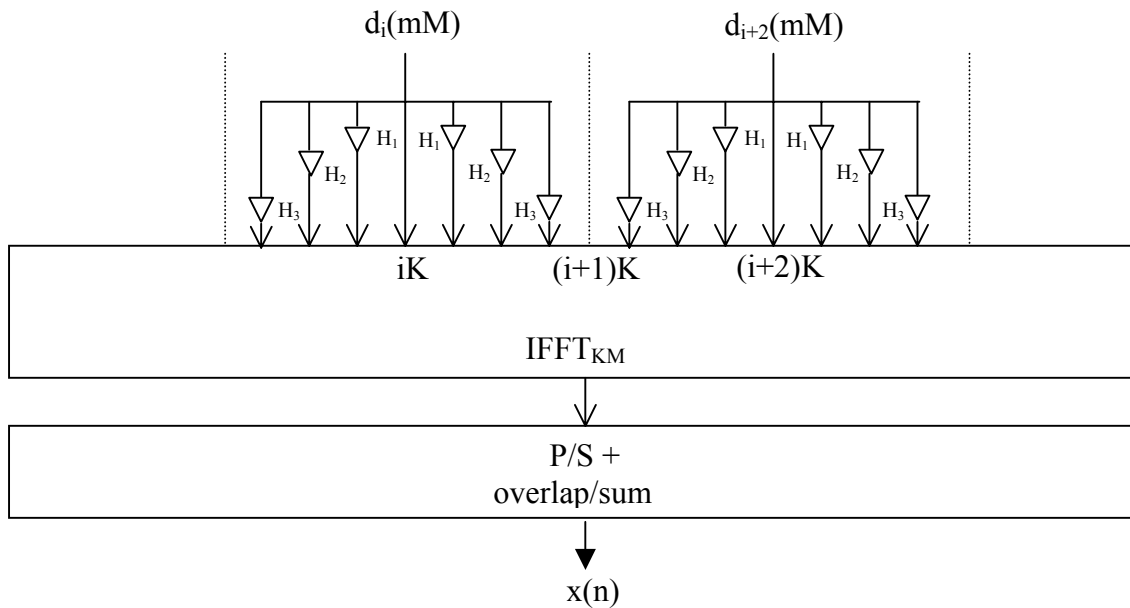


Fig.10. Weighted frequency spreading and extended iFFT

shows that the sub-channels with indices  $i$  and  $i+2$  are separated and do not overlap. On the contrary, sub-channel  $i+1$  overlaps with both and orthogonality is necessary. It is provided by using real inputs of the iFFT for  $i$  and  $i+2$ , and imaginary inputs for  $i+1$ , or the inverse.

The implementation of the receiver is based on an extended FFT, of size  $KM$ . In that case, the FFT input blocks overlap, it is the classical sliding window situation. At the output of the FFT, the data elements are recovered with the help of a weighted despreading operation whose details are given in Fig.11. In fact, the data recovery rests on the following property of the frequency coefficients of the Nyquist filter

$$\frac{1}{K} \sum_{k=-K+1}^{K-1} |H_k|^2 = 1$$

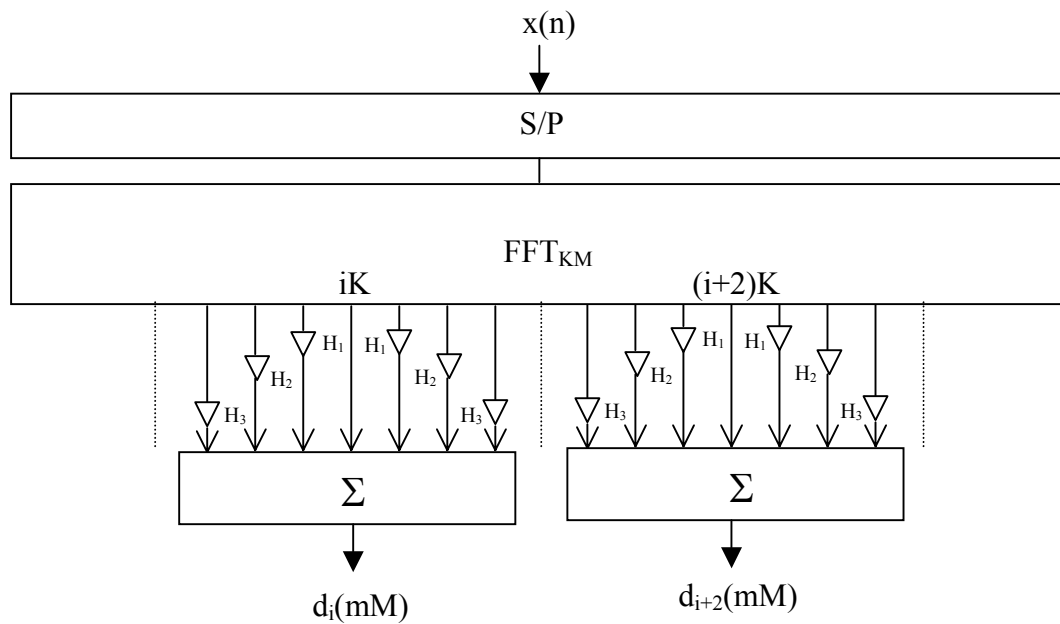


Fig.11. Extended FFT and weighted despreading in the filter bank-based receiver

When the transmitter and the receiver are connected back to back, the delay of the system is  $KM$  transmitted samples, or  $K$  multicarrier symbols.

A remarkable feature of the scheme presented is its simplicity : it is just the scheme of Fig.1 completed by minor operations before and after the iFFT and the FFT. In fact, the key difference is the computational complexity, due to the size of the FFT which is increased from  $M$  to  $KM$  and an issue is how to reduce this complexity.

Due to the overlapping in the time domain of the iFFT outputs and FFT inputs, a significant amount of redundancy is present in the computations. An efficient approach to reduce this redundancy is the so-called PPN-FFT scheme.

## 5. PPN-FFT to reduce computational complexity

A frequency domain vision of filter banks has been presented in the previous section. In this section, the equivalent time domain vision is described, with the objective to reduce the computational complexity. In fact, it will be shown that the size of the FFT can be kept to  $M$ , as in Fig.1, but some additional processing is needed, called polyphase network (PPN).

In the time domain, the prototype filter is defined by a set of coefficients and the relationship between input and output sequences, which is

$$y(n) = \sum_{i=0}^{L-1} h_i x(n-i)$$

The filter impulse response, of length  $L$ , is the sequence of coefficients  $h_i$  ( $0 \leq i \leq L-1$ ) and the frequency response is expressed by

$$H(f) = \sum_{i=0}^{L-1} h_i e^{-j2\pi i f}$$

where the sampling frequency is assumed to be unity.

The filter has linear phase if the coefficients are symmetrical and, in this case, the delay is

$$\tau = \frac{L-1}{2}$$

In digital signal processing, and particularly in digital filtering, it is customary to use the Z-transfer function, which generalizes the frequency response and is defined by

$$H(Z) = \sum_{i=0}^{L-1} h_i Z^{-i}$$

The filter frequency response is the restriction of the Z-transfer function to the unit circle, i.e. it is obtained by letting  $Z = e^{j2\pi f}$ .

Now, if we assume, as in the previous section, that the filter length is a product of two factors,  $L = KM$ , the sequence of filter coefficients can be decomposed into  $M$  interleaved sequences of  $K$  coefficients and the Z-transfer function can be expressed as a double summation

$$H(Z) = \sum_{p=0}^{M-1} H_p(Z^M) Z^{-p}$$

with

$$H_p(Z^M) = \sum_{k=0}^{K-1} h_{kM+p} Z^{-kM}$$

It turns out that each individual filter element,  $H_p(Z^M)$ , has the frequency response of a phase shifter, hence the name of polyphase decomposition, and polyphase network for the complete set.

Now, turning to the filter bank in the transmitter, which is generated by shifting the response of the prototype filter on the frequency axis, a global Z-transfer function can be derived. Shifting the frequency response of the filter  $H(f)$  by  $1/M$  on the frequency axis leads to the function

$$B_1(f) = H\left(f - \frac{1}{M}\right) = \sum_{i=0}^{L-1} h_i e^{-j2\pi i (f-1/M)}$$

The corresponding Z-transfer function is

$$B_1(Z) = \sum_{i=0}^{L-1} h_i e^{j2\pi i / M} Z^{-i}$$

and it is expressed in terms of the polyphase decomposition by

$$B_1(Z) = \sum_{p=0}^{M-1} e^{j\frac{2\pi}{M} p} Z^{-p} H_p(Z^M)$$

The key point here is that the functions  $H_p(Z^M)$  are not affected by the frequency shift. Then, considering all the shifts by multiples of  $1/M$  and the associated filters, and letting  $W = e^{-j2\pi/M}$ , a matrix equation is obtained

$$\begin{bmatrix} B_0(Z) \\ B_1(Z) \\ \vdots \\ B_{M-1}(Z) \end{bmatrix} = \begin{bmatrix} 1 & 1 & \dots & 1 \\ 1 & W^{-1} & \dots & W^{-M+1} \\ \vdots & \vdots & \ddots & \vdots \\ 1 & W^{-M+1} & \dots & W^{-(M-1)^2} \end{bmatrix} \begin{bmatrix} H_0(Z^M) \\ Z^{-1}H_1(Z^M) \\ \vdots \\ Z^{-(M-1)}H_{M-1}(Z^M) \end{bmatrix}$$

The square matrix is the matrix of the inverse discrete Fourier transform (iDFT) and all the filters in the bank have the same filter elements  $H_p(Z^M)$ .

In the implementation, the transmitter output is the sum of the outputs of the filters of the bank. Thus, the processing associated with the filter elements  $H_p(Z^M)$  can be carried out after the summation which is performed by the iDFT. Finally, the structure for the implementation of the filter bank in the transmitter is shown in Fig.12.

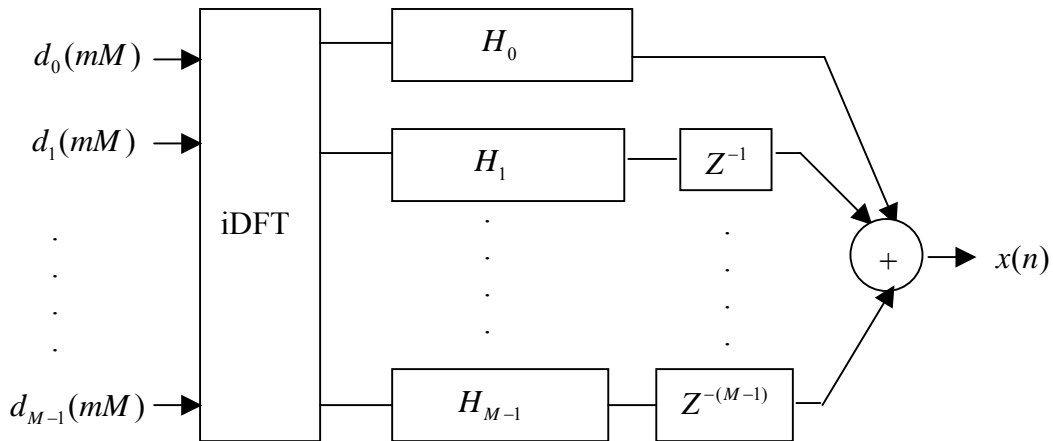


Fig.12. PPN-iFFT implementation of the transmitter filter bank

The same scheme applies to the filter bank in the receiver. The difference is that the frequency shifts are multiples of  $-1/M$  and the discrete Fourier transform (DFT) replaces the iFFT. In fact, for each sub-channel, the signal of interest is shifted around the frequency origin and filtered. Again, the filter elements are the same for all the filters in the bank and, since it is the sum of the sub-channel signals which is received, the processing can be common and the separation of the signals can take place afterwards, with the help of the DFT.

The block diagram of the transmission system is shown in Fig.13. Of course, in practice, the size of the DFT is a power of two and the fast Fourier transform algorithm is implemented. The difference in structure between figures 1 and 13 is just the PPN in the transmitter and the receiver. Note that the system delay is  $K$  multicarrier symbol periods, due to the delay of the prototype filter in the transmit and receive filter banks.

In terms of complexity, each section of the PPN has  $K$  multiplications, as shown in Fig.14 for  $K=4$ , and the complete PPN requires  $KM$  multiplications, which is less than the iFFT, as soon as the number  $M$  of sub-channels becomes large.

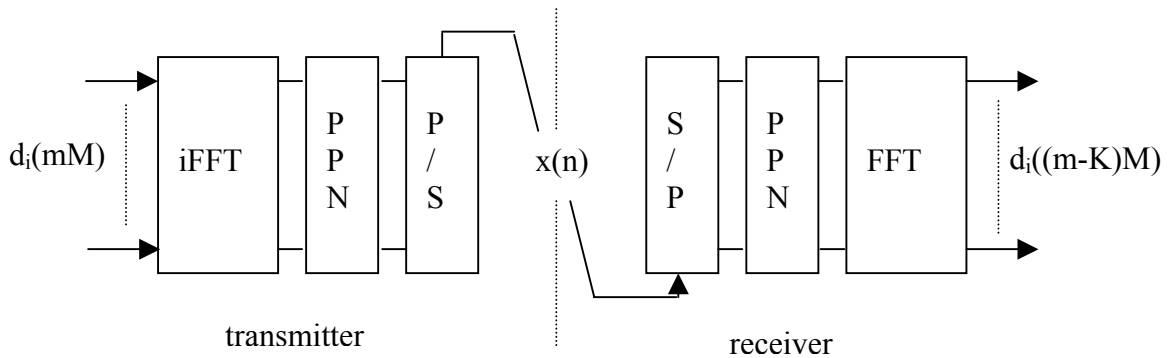


Fig.13. Transmission system using the PPN-FFT scheme

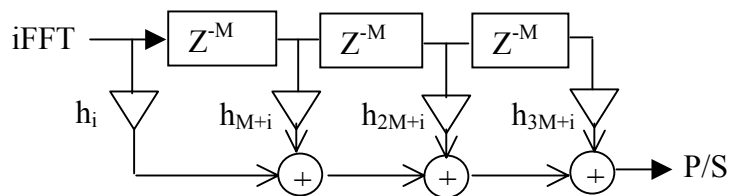


Fig.14. A section of the PPN in the transmitter ( $K=4$ )

The transmitter can generate a real sequence, with almost the same computational complexity. The iFFT size has to be doubled and every input data element  $d_i(mM)$  is applied to two symmetrical inputs. Then, the iFFT output is real and, since the PPN coefficients are real, the transmitter output is real. The receiver can process real signals, with similar changes.

## 6. OQAM modulation

In FBMC systems, any kind of modulation can be used whenever the sub-channels are separated. For example, if only the sub-channels with even (odd) index are exploited, there is no overlap and QAM modulation can be employed. However, if full speed is sought, all the sub-channels must be exploited and a specific modulation is needed to cope with the frequency domain overlapping of the neighbouring sub-channels.

Two important aspects of the transmission systems have been pointed out in sections 3 and 4

- 1) due to the overlapping of neighbouring sub-channels, orthogonality is needed. It is achieved by using the real part of the iFFT inputs with even index and the imaginary part of the iFFT inputs with odd index. But this implies a reduction of the capacity by the factor 2. In fact, full capacity can be restored with the second aspect.
- 2) Due to the symmetry of the transmitter and receiver filters and the fact that they are identical, the imaginary part of the impulse response of the sub-channel interference filter crosses the time axis at the integer multiples of the symbol period and the real part crosses the time axis at the odd multiples of half the symbol period. The time axis crossings are interleaved, as explained at the end of section 3.

Then, the strategy to reach full capacity is the following: double the symbol rate and, for each sub-channel, use alternatively the real and the imaginary part of the iFFT. This way, the real and the imaginary part of a complex data symbol are not transmitted simultaneously as in OFDM, but the imaginary part is delayed by half the symbol duration. The scheme is fully explained by considering the impulse response of the transmitter-receiver cascade.

The most significant part of the impulse response of the transmission system is given in Table 2, for the prototype filter with overlapping factor  $K = 4$ . The time unit is half the inverse of the sub-channel spacing, that is  $T/2$ . It is observed that in sub-channel with index “i”, all the terms are real and the Nyquist criterion is reflected by the zeros. In sub-channels “i-1” and “i+1”, real and imaginary terms alternate, the terms which are simultaneous to the reference term “1” being real. Therefore, from this table, it appears that

- data can be transmitted on the real part of sub-channel  $i$  at sub-channel spacing rate,
- data can be transmitted on the imaginary part of sub-channel  $i$  at sub-channel spacing rate and with a unit time shift,
- the same scheme can be applied for transmission in the neighbouring sub-channels  $i+1$  and  $i-1$ , provided the real and imaginary parts are interchanged.

This is the so-called offset quadrature amplitude modulation (OQAM) and the term ‘offset’ reflects the time shift of half the inverse of the sub-channel spacing between the real part and the imaginary part of a complex symbol. Note that this type of modulation is used in single carrier systems, to improve the peak factor. In the present multicarrier context the throughput rate is the same as with QAM modulation, employed for example in OFDM systems, but without the guard time.

time sub-ch.	p-4	p-3	p-2	p-1	p	p+1	p+2	p+3	p+4
i-1	0.005	j 0.043	-0.125	-j0.206	0.239	j 0.206	-0.125	-j0.043	0.005
i	0	-0.067	0	0.564	<b>1</b>	0.564	0	-0.067	0
i+1	0.005	-j.043	-0.125	j 0.206	0.239	-j 0.206	-0.125	j 0.043	0.005

Table 2. Impulse response of the filter bank transmission system ( $K=4$ )

As concerns implementation, the extended FFT approach of section 4 can be used. The rate is doubled and, in the transmitter, consecutive blocks of  $M$  output samples overlap and the overlapping parts with  $M/2$  samples are added. In the receiver, the FFT window slides by  $M/2$  samples instead of  $M$  samples.

The PPN-FFT approach requires two chains, or a single FFT running at double rate and two PPN devices, as shown in Fig.15 for the transmitter. As mentioned above, the blocks of  $M$  output samples coming out of PPN1 and PPN2 overlap by  $M/2$  samples and an addition is introduced, as shown in the figure.

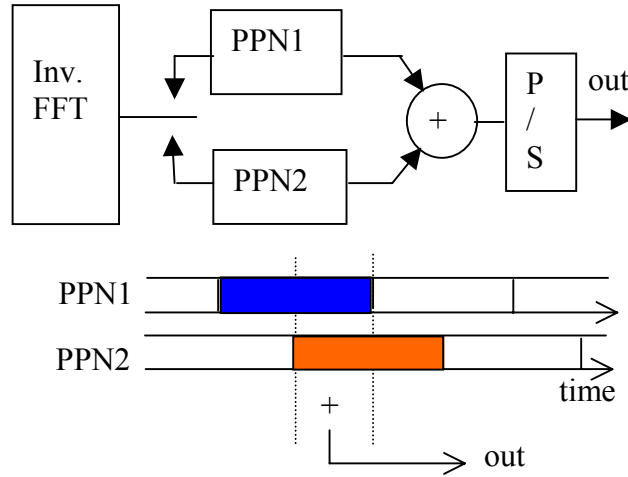


Fig.15. An OQAM transmitter using the iFFT-PPN scheme

At this stage, an important aspect of the OQAM modulation is worth emphasizing, because it will impact some of the functions of the transmission system and, particularly, some applications of the MIMO concept. Let us consider Fig.13 and the output of the FFT in the receiver. Using the notations of Table 2, the signal  $y_i(p)$  coming out of sub-channel  $i$  at time  $p$  contains the useful data element either in its real or imaginary part, and the other part is an interference term determined by the impulse response as in Table 2. Assuming the data element is in the real part, the output signal is expressed by

$$y_i(p) = d_i(p) + j u_i(p)$$

In this expression,  $d_i(p)$  is the desired data element and  $u_i(p)$  is an interference sample expressed in terms of the impulse response coefficients and the neighbouring data elements by

$$u_i(p) = \sum_{l=-1}^1 \sum_{k=-(2K-1)}^{2K-1} c_{lk} d_{i+l}(p-k) \quad ; \quad k, l \neq 0$$

The coefficients  $c_{lk}$  involved in the above expression have the following property

$$\sum_{l=-1}^1 \sum_{k=-(2K-1)}^{2K-1} |c_{lk}|^2 = 1 \quad ; \quad k, l \neq 0$$

Therefore, the power of the interference terms equals the power of the data elements, assumed statistically independent. The histogram of their amplitudes is shown in Fig.16 for binary data and  $K=4$ .

The interference terms and their amplitude distribution have an impact on some of the system functions, such as pilot detection and MIMO processing.

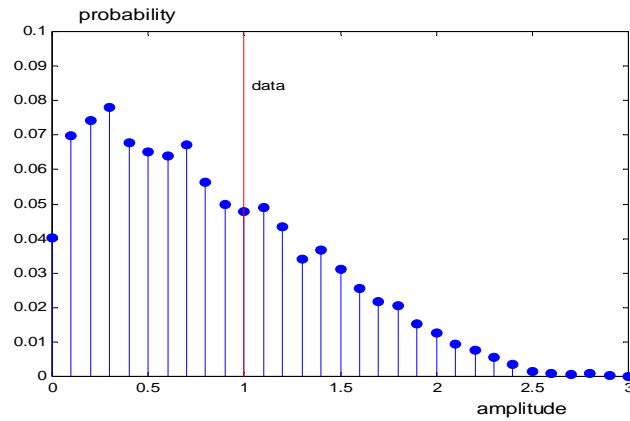


Fig.16. Histogram of the amplitudes of the interference terms

## 7. Effects of the transmission channel

In transmission systems, a channel is inserted between the transmitter and the receiver and it introduces a number of impairments, such as amplitude and phase distortion, timing offset, frequency offset and noise. The impact of these impairments and the way to counter them in the multicarrier context depend on how the multicarrier system is exploited. A feature of FBMC is that independent groups of sub-channels can be allocated to different users and user synchronization is not mandatory, although beneficial if realized.

As can be seen in Fig.7, in order to make two groups of sub-channels independent and make full usage of the spectrum, it is sufficient to introduce an empty sub-channel in-between.

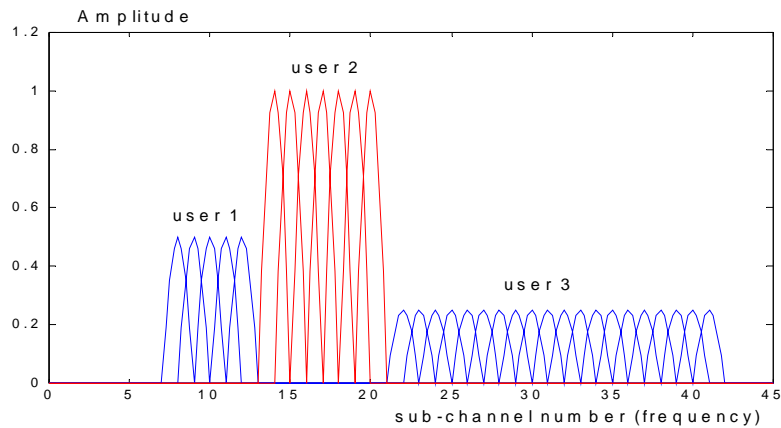


Fig.17. Spectra of multi-user signals received by a mobile radio base station

The most challenging situation occurs in the uplink of a radio network, when the signals coming from different mobile users reach the base station with different attenuations, timing offsets and frequency offsets. An illustration is given in Fig.17, where 3 users with different needs are allocated 4, 7 and 20 sub-channels. In this situation, the base station has access to the outputs of the sub-channels only and the compensation of the channel impairments must be performed at this level.

In the sub-channel with index  $i$ , at the frequency  $i/M$ , the amplitude and phase distortion of the channel introduce the factor  $A(i/M)e^{j\phi(i/M)}$ . The contribution of the timing offset  $\tau$  is

the factor  $e^{-j2\pi\tau i/M}$ . As for the frequency offset  $\delta f$ , it introduces a phase shift proportional to time and expressed by  $e^{j2\pi\delta f mM}$ .

In fact, due to the direct dependence on the time and the change at each symbol, the frequency offset is subject to a separate treatment. First, it is measured, for example at initialization, with the help of a particular signal, generally made of two or more identical parts to neutralize the other effects. Then, it is compensated, at the sub-channel output, by a phase rotation which is incremented at each multicarrier symbol. The other effects, amplitude and phase distortion, timing offset and some residual distortion due to the frequency offset, can be compensated through a sub-channel equalizer.

In the field of equalization, the fractionally spaced equalizer, since its invention more than three decades ago, is recognized as providing the best performance and the highest efficiency. In fact, with the symbol rate, or baud-spaced, equalizer, due to the Nyquist symmetry around the cut-off frequency, aliasing occurs and the in-band signal and the aliased signal add constructively only if time alignment is achieved, otherwise part of the spectrum is distorted or lost. Therefore, the baud-spaced equalizer requires time alignment. On the contrary, if the sampling rate of the equalizer is doubled, then there is no spectrum aliasing, provided the prototype filter roll-off is at most equal to the sub-channel spacing, and equalization can be achieved in the presence of timing offset.

The capability to cope with timing offsets is crucial for some situations in radiocommunications, such as the uplink in base station ruled networks, but, also, in the opportunistic unsynchronized networks of cognitive radio, where the spectrum access must be achieved as quickly as possible and with the maximal flexibility.

## 8. Sub-channel equalization

The sub-channel equalizer can be implemented in the frequency domain or in the time domain, depending on the receiver filter bank implementation.

The introduction of the equalizer in the extended FFT approach is shown in Fig.18.

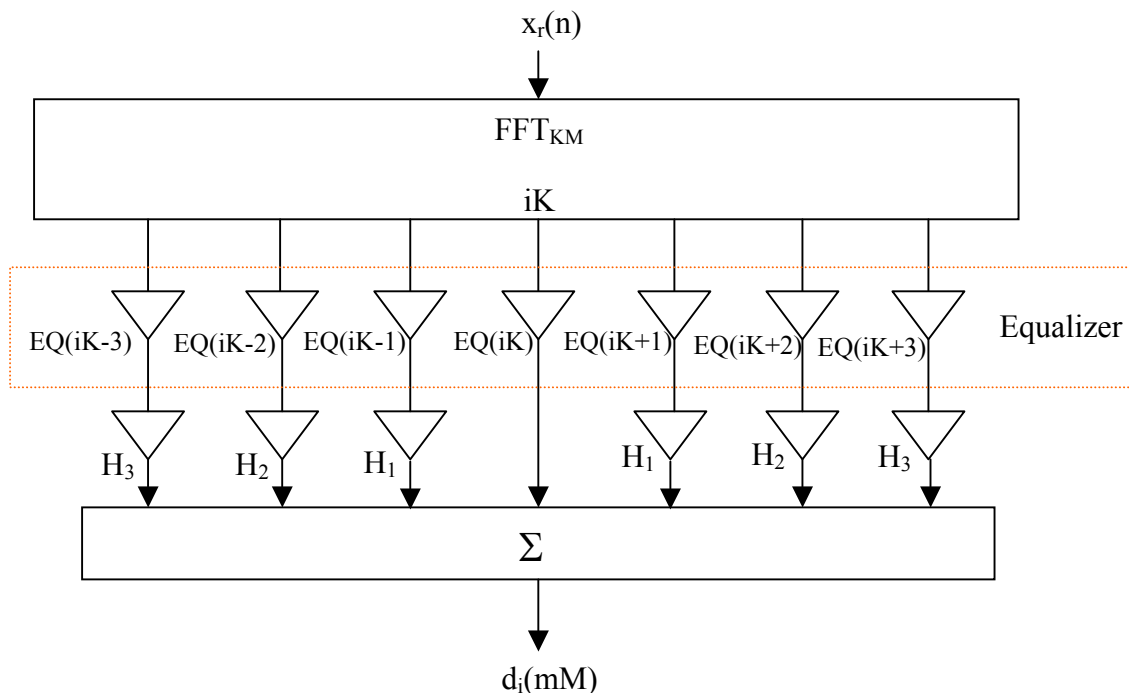


Fig.18. Frequency domain sub-channel equalizer

Actually, with this perspective, the system exploits  $2K-1$  sub-carriers per sub-channel and equalization is required at the frequencies of these  $2K-1$  sub-carriers.

The frequency coefficients  $EQ(iK+k), -K+1 \leq k \leq K-1$  are determined from the measurements of the transmission channel. For example, if the channel has been measured with the frequency spacing  $1/KM$ , assuming no frequency offset and no noise, the equalizer coefficients are just the inverse of the measured values

$$EQ(iK+k) = 1/C(iK+k)$$

If the frequency spacing of the channel measurements is  $1/M$ , as in OFDM, then the desired  $KM$  values can be obtained through interpolation. As for the frequency offset, it can be compensated by a frequency shift at the output of the frequency despreading device.

It is worth emphasizing that equalization requires no additional delay with this scheme and virtually no additional arithmetic operations, since equalization and filtering can be merged.

In the PPN-FFT approach, the sub-channel equalization takes place in the time domain. The simplest structure is the transversal equalizer whose coefficients are derived from the frequency measurements by inverse DFT. Specifically, the set of  $2K-1$  frequency coefficients  $EQ(iK+k)$  is completed by the value

$$A = EQ(iK - K + 1) - EQ(iK - K + 2) + \dots + EQ(iK + K - 1)$$

and an inverse DFT of size  $2K$  is calculated. The  $2K-1$  non-zero values obtained are the time domain equalizer coefficients. Such an equalizer introduces the delay  $\Delta = K - 1$  symbols.

The block diagram of the time domain equalizer for the sub-channel with index  $i$  is shown in Fig.19. The frequency offset is compensated by a complex multiplication at the FFT output. The transversal equalizer  $He(Z)$  delivers the output signal with the additional delay  $\Delta$ .

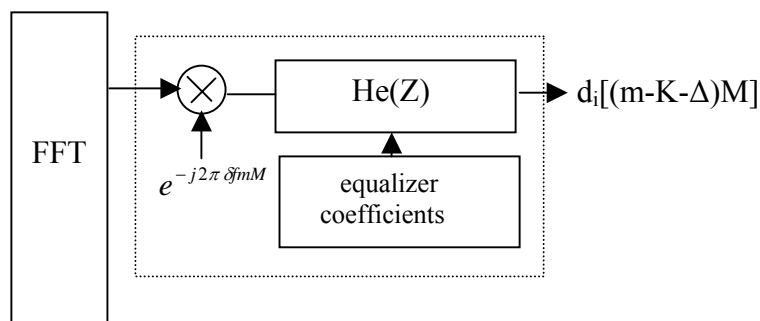


Fig.19. Time domain sub-channel equalizer in the receiver

It must be pointed out that the length of the equalizer  $He(Z)$  depends on the transmission channel and it may be less than  $2K-1$ , which reduces the delay and the computational complexity, at the cost of a possible performance degradation. In fact, it is the timing offset compensation which may lead to large values, because of the interpolation involved, and a rule of the thumb for choosing the equalizer length  $Leq$  is as follows

- moderate amplitude and phase distortion, no timing offset:  $Leq = 1$  ,
- severe amplitude and phase distortion, timing offset up to 10 % of its maximum value:  $Leq = 3$  ,
- timing offset up to its maximum value (  $T/4$ ):  $Leq$  up to  $2K-1$ . Such a situation may occur at the base station when the distant mobile users are not synchronized.

The characteristics of the transmission channel may change with the time. In that case, the equalizer coefficients can be updated periodically, from measurements obtained with the help of pilot multicarrier symbols or known data elements in some symbols, the so-called scattered pilots. Alternatively, continuous updating can be implemented using adaptive techniques, to track the channel variations.

It is worth pointing out that the detection of scattered pilots leads to specific operations, due to the OQAM modulation. The measurement of the amplitude and phase in a given sub-channel requires two values, which are obtained not simultaneously but at consecutive times. Referring to section 6, let us assume that the pilot data elements “1” occur at times  $p$  and  $p+1$  in the sub-channel under consideration. In the absence of distortion in the transmission channel, the signal at the output of the receiver filter bank is

$$x(p) = 1 + ju(p) \quad ; \quad x(p+1) = u(p+1) + j$$

In the presence of channel distortion, the received samples are  $y(p)$  and  $y(p+1)$ . The equalizer complex coefficient  $h = h_r + jh_i$  is such that

$$[y_r(p) + jy_i(p)][h_r + jh_i] = 1 + ju(p) \quad ; \quad [y_r(p+1) + jy_i(p+1)][h_r + jh_i] = u(p+1) + j$$

The solution of this system is

$$\begin{bmatrix} h_r \\ h_i \end{bmatrix} = \frac{1}{y_r(p)y_r(p+1) + y_i(p)y_i(p+1)} \begin{bmatrix} y_r(p+1) + y_i(p) \\ -y_i(p+1) + y_r(p) \end{bmatrix}$$

In the presence of noise, it can be shown that the noise terms are divided by the quantity  $u(p) + u(p+1)$ , which is beneficial if the magnitude of the divider is greater than unity, but a penalty otherwise. A simple way to increase the magnitude of the divider is to multiply the amplitude of the pilot samples by a factor of a few units, e.g. 2 or 3.

An alternative approach is the so-called interference cancellation method (ICM), which leads to the same detection operation as QAM. Referring to Table 2, the interference sample  $u(p)$  is cancelled by choosing appropriately the second or “auxiliary” pilot. This requires the knowledge of the data values involved in the expression of  $u(p)$  and, therefore, a delay of  $K-1$  multicarrier symbols is introduced in the transmitter.

## 9. Burst transmission with FBMC

The performance of FBMC systems in burst transmission is impacted by the length of the impulse response of the prototype filter.

Let us assume that  $N_s$  multicarrier symbols have to be transmitted in a burst. With FBMC, the emitted burst begins with the first signal sample associated with the first symbol and it finishes with the last signal sample associated with the last symbol. Due to the overlapping factor  $K$ , the length of the burst is increased by  $K-1$  symbol periods, compared to a scheme with no overlapping, such as OFDM. An FBMC burst is shown in Fig.20, for  $K=4$ . The initial and final transition phases are both equal to  $(K-1)/2$  symbol periods. The impact is a reduction of the transmitted data for a given length of the burst, which is not negligible for some contexts such as time division duplex (TDD) with short bursts. It is clear from the figure that, the signal in some parts of the transitions is very small and some cut-offs are possible with

minor degradations. However, if the spectra of adjacent users must be fully preserved, it is necessary to keep the entire transitions. Conversely, if a user is separated from the neighbouring users by spectral gaps, then the transitions can be shortened, with the corresponding increase in data rate.

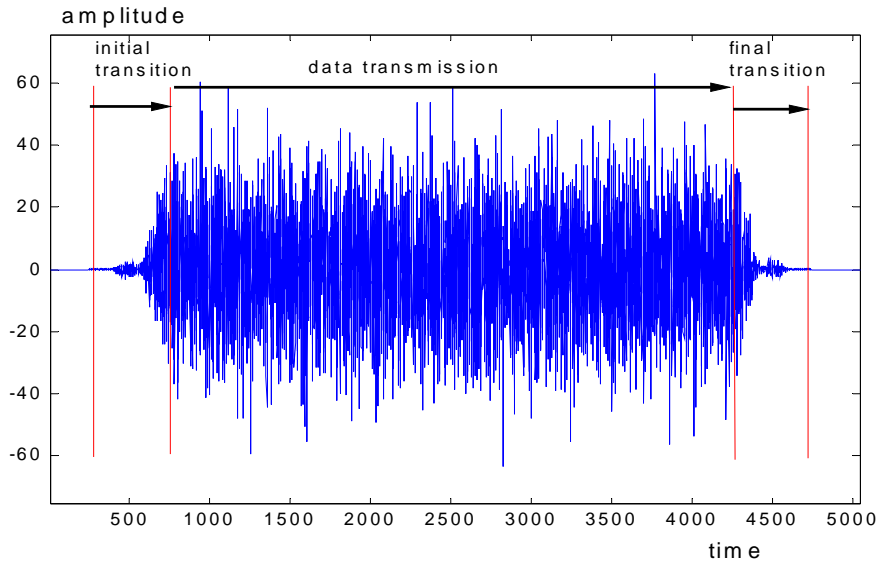


Fig.20. Structure of the transmitted burst with FBMC

When the burst begins with a preamble for the estimation of the channel parameters, the filter impulse response may have to be taken into account in the transition between preamble and data symbols. In fact, if accurate measurements are expected in the initialization phase, the data signals should not interfere with the preamble signals. An illustration is provided in Fig.21, where the initialization phase and the data transmission phase are represented by the signals at the output of the receiver.

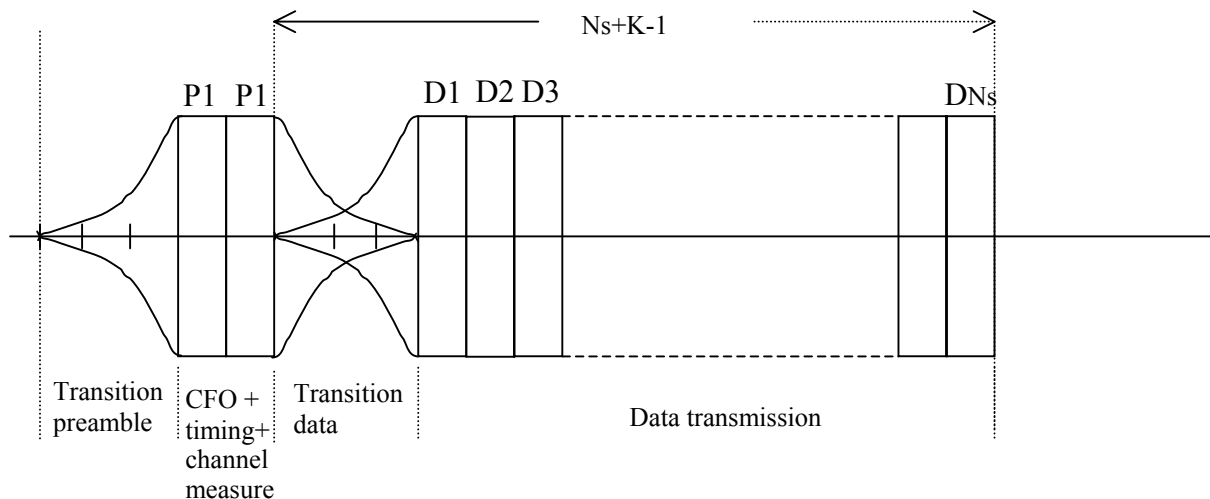


Fig.21. FBMC burst with preamble and data transmission, at the receiver output

The preamble sequence of 2 symbols (P1) requires a transition of  $K-1$  symbol periods, so that the channel measurements are carried out with a stationary signal. Then, the rising phase of

the data sequence and the decaying phase of the preamble are superimposed. In total, the transmission of 2 preamble symbols and  $N_s$  data symbols requires a transmitted burst length of  $2+N_s+2(K-1)$  symbol periods with this scheme. Again, some shortenings of the transitions can be contemplated, in relation with the spectral context and the performance objectives.

### Example

An FBMC system exploiting OQAM modulation has the parameters :  $L=1024$ ,  $M=256$ ,  $K=4$ . When the first 384 samples of a burst are deleted, the system impulse response results from the cascade of the truncated transmit filter and the full receive filter and it is given in Table 3, where 4 adjacent sub-channels are considered.

Sub-channel	i	i+1	i+2	i+3
Time p-4	0.001	- 0.001 j	-0.001	0
p-3	-0.029 - 0.001 j	-0.005 -0.024 j	0.004 -0.006j	0.001 -0.004j
p-2	0.001 - 0.005 j	-0.061 -0.053 j	-0.001 +0.030j	0.001 -0.019j
p-1	0.493 - 0.012 j	-0.078 +0.259 j	-0.023 +0.060j	-0.011+0.042j
(Reference) p	<b>0.971 + 0.005 j</b>	0.259 <b>-0.012 j</b>	<b>-0.015 +0.018j</b>	0.007 <b>-0.016j</b>
p+1	0.572 - 0.001 j	<b>0.006 -0.210 j</b>	0.002 <b>-0.006j</b>	<b>0.001 -0.004j</b>
p+2	0	-0.125	0	0
p+3	-0.007	0.043 j	0	0
p+4	0	0.005	0	0

Table 3. System impulse response when the first 384 samples of the transmit filter impulse response are deleted

A comparison with Table 2 shows the effects of the cut, namely intersub-channel interference for the first OQAM symbol of the burst. The interference terms are marked in red.

Now, different cuts are considered and the results are given in Table 4. For example, when the first 384 samples of the burst are cut, the signal-to-interference ratio is  $SIR= 27$  dB for the first half of the first OQAM symbol,  $S1/1$ , it is 38 dB for the second half,  $S1/2$ , and it is 63 dB for the first half of the second symbol  $S2/1$ . The consequence is that, if the OQAM constellation has the size 256 for example, i.e. the first and the second half of a symbol carry 4 bits each, the first half of the first symbol has to be limited to 3 or 2 bits, while the second half and the subsequent symbols may carry the full load. The same reasoning applies to the last symbol in the burst, when the last 384 samples of the burst are deleted.

Nb.of coeff. cut	256	320	384	448
SIR (dB) - S1/1	47	47	27	13
- S1/2	65	59	38	33
- S2/1	65	65	63	37

Table 4. Impact of burst cuts on the first and last symbols.

From Table 4, it appears that no reduction in bit loading is required for cuts of 320 and 256 samples, while a cut of 448 samples leads to the loss of half an OQAM symbol.

Regarding the total length of the FBMC burst, the delay  $T/2$ , half a symbol duration, between the first and the second half of the OQAM symbol must be taken into account. With cuts of

384 samples at both ends, the length of the FBMC/OQAM burst to transmit  $N_s$  symbols is  $(N_s+1/2)T$ , which is just  $T/2$  more than OFDM.

An important information provided by Table 3 is related to the precursors, the samples which precede the reference sample. When a system operates in a dense spectral environment, the burst cuts cause temporary interferences to the adjacent unsynchronized users. The maximum interference level, in sub-channel  $i+2$  at time  $p-1$ , is  $-24$  dB. Of course, similar effects are observed with the bursts in OFDM systems.

## 10. MIMO – FBMC

Multi-input Multi-output (MIMO) techniques combine nicely with multicarrier transmission, particularly OFDM, and sophisticated algorithms have been developed in that context. As pointed out above, a key characteristic of FBMC is the possibility to have independent (non overlapping) sub-channels. Therefore, two situations may occur in FBMC transmission for the application of the MIMO concepts

- the sub-channels do not overlap, which occurs when a user exploits a single sub-channel or non-adjacent sub-channels. Then, QAM modulation can be used, the MIMO context is similar to OFDM and the same techniques can be implemented.
- the subcarriers overlap and offset QAM modulation is used. This situation corresponds to the search for maximum throughput. Then, the OFDM techniques must be adapted and specific schemes must be employed.

The two main approaches of the MIMO concept, namely spatial multiplexing and spatial diversity, can be applied to the FBMC context with OQAM modulation, as described below.

***Spatial multiplexing*** In spatial multiplexing the data throughput is increased by transmitting different streams of data over different antennas. The case of 2 antennas at the transmitter and 2 antennas at the receiver is illustrated in Fig.22.

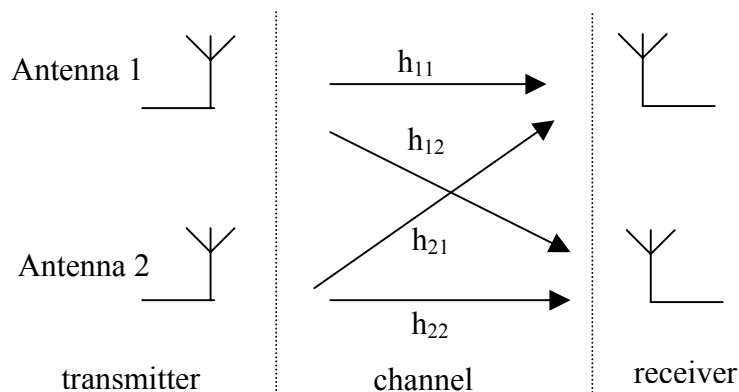


Fig.22. MIMO 2x2 transmission

The transmission channel consists of 4 elementary channels and it is modelled by the matrix

$$H = \begin{bmatrix} h_{11} & h_{21} \\ h_{12} & h_{22} \end{bmatrix}$$

In fact, the elementary channels have some common parameters. In particular, the signals coming out of the transmitter are synchronized in frequency and time. Thus, the signals at the

receiver antennas can be assumed to have the same carrier frequency offset and the same timing offset. As a consequence, it is sufficient to measure these parameters once and use the same equalizers to compensate them in the receiver chains, as depicted in Fig.23. Each antenna is connected to a filter bank and the outputs of the filter banks with the same index are connected to sub-channel equalizers, whose outputs are fed to the common MIMO decoder. In fact, after this sub-channel equalization, only the amplitude and phase of the sub-channel remain to be compensated and they are represented by the matrix  $H$ , in which the elements are complex scalars. These matrix elements are available, for each sub-channel, after the channel measurement phase which has taken place at initialization for example. With such a scheme, the MIMO concept can be extended to unsynchronized distant mobile users.

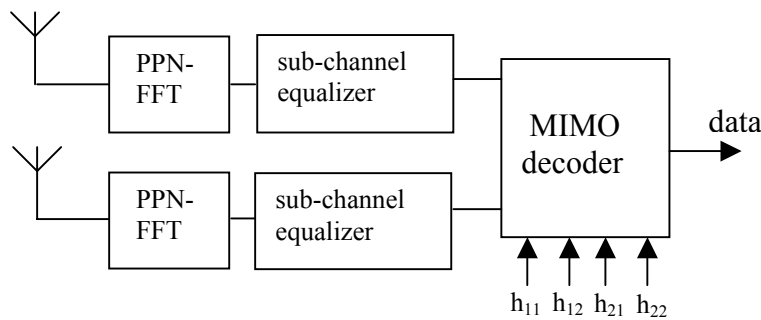


Fig.23. MIMO 2x2 receiver structure

Now, the operation of the MIMO decoder which delivers the data is described. Referring to section 6, for a particular symbol and a particular sub-channel, the signal at the first input of the MIMO decoder is expressed by

$$x_1 = (d_1 + ju_1)h_{11} + (d_2 + ju_2)h_{21}$$

where  $d_1$  and  $d_2$  are the data element transmitted by the first and the second antenna respectively and  $u_1$  and  $u_2$  are the associated interference samples, as explained at the end of section 6. The complex scalars  $h_{11}$  and  $h_{21}$  represent the transmission channel elements at the center frequency of the sub-channel under consideration, assuming perfect frequency and time synchronization after sub-channel equalization. Similarly, the signal at the second input of the MIMO decoder is expressed by

$$x_2 = (d_1 + ju_1)h_{12} + (d_2 + ju_2)h_{22}$$

In theory, the data elements are recovered from the above expressions by the matrix inversion

$$\begin{bmatrix} d_1 \\ d_2 \end{bmatrix} = \text{Re} \left[ \begin{bmatrix} h_{11} & h_{21} \\ h_{12} & h_{22} \end{bmatrix}^{-1} \begin{bmatrix} x_1 \\ x_2 \end{bmatrix} \right]$$

In practice, noise components  $n_1$  and  $n_2$  with power  $\sigma^2$  are added to the signals  $x_1$  and  $x_2$  and the minimum mean square error (MMSE) technique is employed, yielding the following estimations

$$\begin{bmatrix} \tilde{d}_1 + j\tilde{u}_1 \\ \tilde{d}_2 + j\tilde{u}_2 \end{bmatrix} = GH \begin{bmatrix} d_1 + ju_1 \\ d_2 + ju_2 \end{bmatrix} + G \begin{bmatrix} n_1 \\ n_2 \end{bmatrix}$$

with

$$G^t = (H^* H^t + \sigma^2 I_2)^{-1} H^*$$

The maximum likelihood (ML) techniques are simplified with OQAM modulation because the data are real, but they can be applied only once the interference terms  $u_1$  and  $u_2$  have been subtracted from the received signals. These terms can be derived from the above MMSE equations, taking the imaginary part of the estimated vector. Alternatively, they can be calculated according to their definition given in section 6, in which the data terms are replaced by estimations. Note that, in the latter case, a delay is introduced in the ML detection process.

**Spatial diversity** Diversity can be implemented in the time domain or in the frequency domain and at the transmitter or at the receiver. There is nothing specific with FBMC for receive diversity. However, for transmit diversity, which is important in downlink radio for example, the OQAM modulation introduces specific constraints, due to the presence of the interference term besides the useful term in every complex sample coming out of the receiver filter bank. The interference term has to be separated from the data in the diversity processing. Again the case of 2 antennas is considered and it is illustrated in Fig.24.

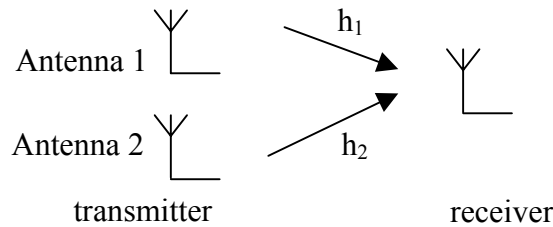


Fig.24. Transmit diversity with 2 antennas

A first approach is delay diversity and it consists of transmitting the same sequence from the two antennas but with a delay. In this case, the MIMO 2x1 channel is modelled by a 2-tap FIR filter, as shown in Fig.25.

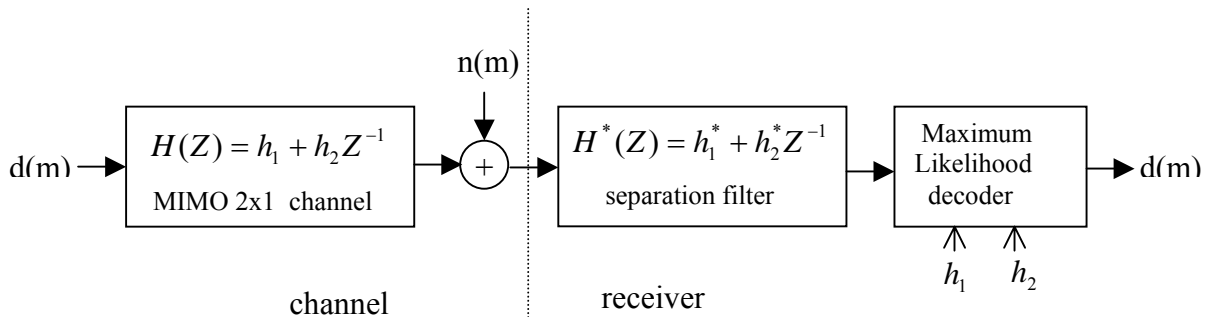


Fig.25. Model of transmit diversity MIMO 2x1

The sequence of data  $d(m)$  is assumed real and, taking into account the interference sequence  $u(m)$ , the received signal is expressed by

$$x(m) = h_1(d(m) + ju(m)) + h_2(d(m-1) + ju(m-1))$$

Since the filter coefficients  $h_1$  and  $h_2$  are assumed to be complex scalars, the real data and the interference samples are mixed up and they must be separated, which is achieved by the

conjugate of the channel filter. Then, at the output of the separation filter, the received signal is given by

$$y(m+1) = h_1^* x(m+1) + h_2^* x(m)$$

or

$$y(m+1) = |h_1|^2 (d(m+1) + ju(m+1)) + [h_1^* h_2 + h_2^* h_1] (d(m) + ju(m)) + |h_2|^2 (d(m-1) + ju(m-1))$$

Then, a sequence free of interference is obtained by

$$\text{Re}(y(m+1)) = |h_1|^2 d(m+1) + 2 \text{Re}(h_1 h_2^*) d(m) + |h_2|^2 d(m-1)$$

In practice, a noise sequence  $n(m)$  is added to the received signal, as shown in Fig.25. Then, the data are retrieved through conventional techniques, such as decision feedback equalization or maximum likelihood (ML) decoding. However, concerning ML decoding, it must be noticed that the received noise sequence is filtered to produce the noise component accompanying  $y(m)$ . Therefore, this noise component is correlated and the ML technique yields sub-optimal results. In fact, the noise filter has to be included in the calculation of the equivalent signal-to-noise ratio (SNR) of the ML decoder and iterative techniques must be employed to reach a value close to the full diversity SNR which is expressed by

$$SNR_{div} = \frac{|h_1|^2 + |h_2|^2}{\sigma^2}$$

The extension to more than 2 antennas of the transmit time diversity technique presented above leads to channel filters with more than 2 taps and the processing is modified accordingly.

With QAM modulation, the full diversity SNR is reached by the so-called Alamouti scheme which consists of transmitting consecutive data in pairs as follows

$$\text{antenna 1: } [d_1, -d_2^*] \quad ; \quad \text{antenna 2: } [d_2, d_1^*]$$

Then, the received samples are

$$x_1 = h_1 d_1 + h_2 d_2 + n_1 \quad ; \quad x_2 = -h_1 d_2^* + h_2 d_1^* + n_2$$

and the decision variables are obtained by

$$\begin{aligned} \tilde{d}_1 &= h_1^* x_1 + h_2 x_2^* = (|h_1|^2 + |h_2|^2) d_1 + h_1^* n_1 + h_2 n_2^* \\ \tilde{d}_2 &= h_2^* x_1 - h_1 x_2^* = (|h_1|^2 + |h_2|^2) d_2 + h_2^* n_1 + h_1 n_2^* \end{aligned}$$

This scheme cannot be applied to OQAM symbol-wise, due to the presence of the interference terms. However, it can be applied block-wise.

Let us consider 2 sets of N data elements  $[d_{11}, d_{12}, \dots, d_{1N}]$  and  $[d_{21}, d_{22}, \dots, d_{2N}]$ . As explained in section 6 about OQAM modulation, the data samples allocated to a given sub-channel are applied alternatively on the corresponding real and imaginary input of the

synthesis filter bank. Changing the signs of the data applied to the imaginary inputs is equivalent to complex conjugation and the corresponding sequence is denoted  $[d_{11}^*, d_{12}^*, \dots, d_{1N}^*]$ . Now, a property of the filter bank impulse response, as shown in Table 2 of section 6, is that reversing the time leads to complex conjugation. Thus, if the sequence  $[d_{1N}^*, \dots, d_{12}^*, d_{11}^*]$  is applied to the system, the conjugate time-reversed version of the output is the same as the output produced by applying the original sequence. Then, the block Alamouti scheme consists of transmitting consecutive blocks as follows

$$\begin{array}{ll} \text{Antenna 1} & [d_{11}, d_{12}, \dots, d_{1N}] \quad [-d_{2N}^*, \dots, -d_{22}^*, -d_{21}^*] \\ \text{Antenna 2} & [d_{21}, d_{22}, \dots, d_{2N}] \quad [d_{1N}^*, \dots, d_{12}^*, d_{11}^*] \end{array}$$

and performing the decoding as above, using the conjugate time-reversed version of the second block received. In the process, the data and interference samples are separated, as in the delay diversity approach described earlier in this section. Of course, a guard time must be introduced between the blocks, as described in the previous section for burst transmission. The following aspects of the block Alamouti scheme are worth pointing out

- a delay equal to twice the block length is introduced in the transmission,
- the transmission channels should not vary significantly during two blocks, which limits the validity of the scheme to low mobility cases.

## 11. Compatibility with OFDM

FBMC systems are likely to coexist with OFDM systems. Since FBMC is, in fact, an evolution of OFDM, some compatibility can be expected.

Compatibility begins at the specification and system parameter level. The sampling frequency is the same and the sub-channel spacing of FBMC is equal to the sub-carrier spacing of OFDM or it is a sub-multiple, so that the FFT is the same, or a subset of the FFT is the same. In OFDM systems, the sub-carriers are integer multiples of the spacing. Similarly, the sub-channels in FBMC systems are centered on the integer multiples of the spacing, as described in the present document.

Compatibility is particularly helpful at initialization, because software defined multimode receivers have to decide reliably which scheme to implement. At the beginning of a packet, the OFDM receiver has to synchronize in frequency and time, and measure the transmission channel, in order to determine the coefficients of the frequency domain equalizers. Generally, several multicarrier symbols, called pilot symbols and grouped in a preamble, are reserved for this task and the FFT is instrumental in the process. The FBMC receiver has to carry out the same functions and it can rely on its FFT to that purpose, so that the techniques and algorithms developed for OFDM are exploited by FBMC. Some complements may be necessary, such as the interpolation mentioned in section 8 above to derive the coefficients of the FBMC multitap equalizer from the OFDM single tap equalizer. Then, it is important to have the possibility to exploit the FFT in the initialization phase without having to reconfigure the terminal, i.e. keeping the structure used for data transmission. A method to reduce the filter bank to the FFT consists of neutralizing, or by-passing, the PPN, which is obtained through the memory preloading technique

The structure of the filter bank in the transmitter is sketched in Fig.26, for K=4. The PPN contains 4 memories in which the block of signal samples issued from the IFFT propagate.

The output signal  $y(n)$  is obtained by a weighted summation of the memory contents. The PPN consists of a set of  $M$  digital filters whose  $K$  coefficients are derived from the prototype filter impulse response through interleaving. In fact, the prototype filter impulse response is decomposed into  $M$  interleaved sequences of  $K$  coefficients each. A remarkable property of these sequences, due to the zeros of the prototype frequency response as mentioned in section 3, is that the sum of the  $K$  coefficients in each interleaved sequence is unity. Thus, to neutralize the PPN, it is sufficient, instead of letting the propagation happen as in Fig.26, to preload the memories of the PPN with the set of samples produced by the IFFT in the transmitter and with the set of received samples to be applied to the FFT in the receiver. With this scheme, the transition phases are cancelled for the preamble and the FFT is operating as in OFDM.

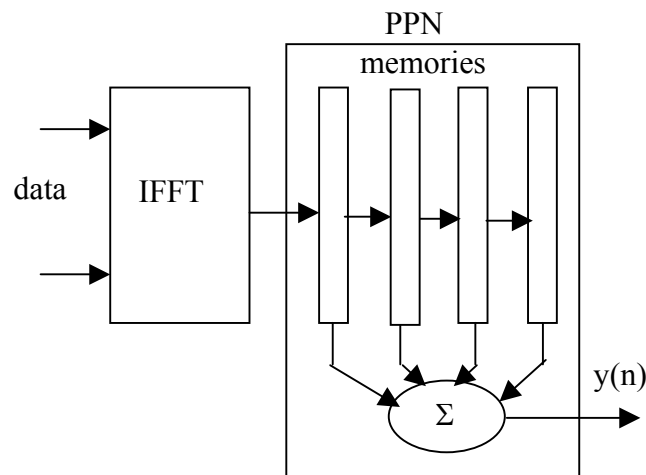


Fig.26. Structure of the transmitter filter bank

With memory preloading, the burst of Fig.21 is modified as shown in Fig.27.

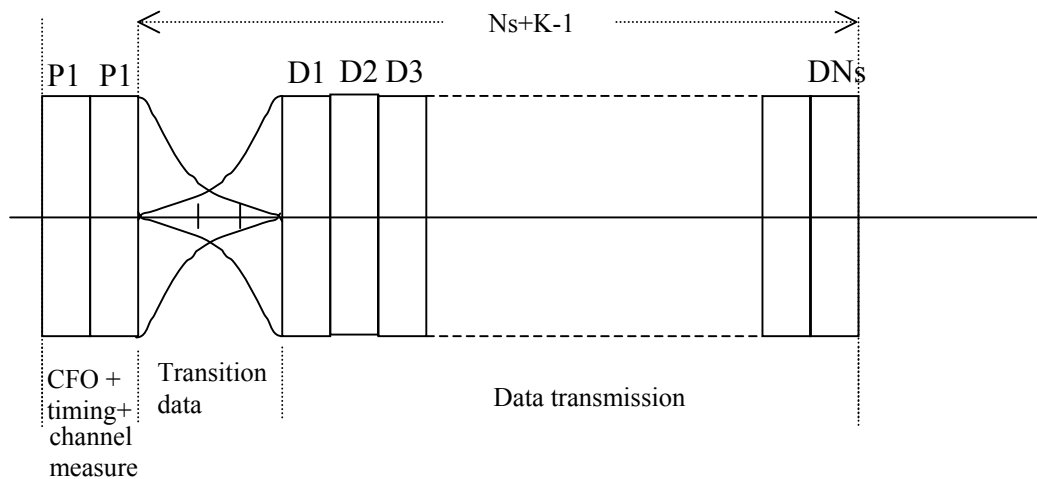


Fig.27. FBMC burst with OFDM compatible initialization

As mentioned in section 9, the transition for data can be shortened. In that case, the first data symbol might not carry the full bit load.

The approach can be extended to the MIMO context, where multiple channel estimations are obtained with the help of multiple preloading operations.

## 12. FBMC in networks

FBMC techniques have the potential to enhance the performance of synchronized conventional networks and add new functionalities. They are an enabling technology for the efficient deployment and the acceptance of opportunistic networks. The following aspects are worth pointing out.

- *Carrier assignment schemes in asynchronous context.* FBMC is a multicarrier technique, like OFDM, and it supports the schemes which have been developed in the context of synchronized networks. But, it can also handle situations where the users are not synchronized. For example, in the uplink of a base station ruled network, it is not necessary to achieve distant frequency and time alignment before starting data transmission. This is due to the fact that users are separated if an empty sub-channel is introduced between the sub-channels or groups of sub-channels they exploit.
- *High density of users.* The minimum spectral distance of unsynchronized neighbouring users is the sub-channel frequency spacing of the FBMC system.
- *Delay and prototype filter impulse response.* The counterpart for the spectral separation provided by the filter banks is the introduction of a delay in the transmission, which, in some applications, must be taken into account when defining the systems and some of their parameters. The round-trip delay of an FBMC system is  $2K$  multicarrier symbol periods, twice the overlapping factor of the prototype filter. In burst transmission, if the spectra of the neighbouring users have to be preserved, initial and final transition times are present and the burst is extended by  $K-1$  symbol periods. Therefore, FBMC favors longer bursts.
- *Efficient usage of the allocated spectrum.* FBMC is a multicarrier transmission technique which requires no cyclic prefix and exploits the totality of the symbol period. Combination of filter banks with OQAM modulation leads to maximum data transmission speed.
- *Robustness to narrow-band jammers and impulse noise.* A high level narrow-band jammer does not kill the multicarrier transmission, it only affects the sub-channels which overlap with the jammer in the frequency domain. The robustness of the multicarrier system to channel impulse noise is significantly enhanced by the presence of the filter banks.
- *Computational complexity.* The additional complexity brought by the filter bank in the FBMC receiver can be expressed taking the FFT of the OFDM receiver as the reference. It depends on the number  $M$  of sub-channels in the system and the overlapping factor  $K$ . Assuming straightforward implementations, for  $M=256$  and  $K=4$ , the filter bank in the FBMC receiver requires roughly 4 times more computations than the FFT of the OFDM receiver if the PPN-FFT scheme is employed and 8 times if the extended FFT scheme is employed. This additional complexity must be put in perspective and what is to be considered is its impact on the complexity of the entire system, including all the functions and, particularly, the iterative data recovering algorithms and error correcting codes.
- *Compatibility OFDM-FBMC.* Both OFDM and FBMC techniques are based on the FFT, and they have a common core. However, due to the presence of the cyclic prefix in OFDM, the streaming of the signals is different. But, whenever the cyclic prefix is not present, for example in initialization phases, compatibility can be ensured.

Cognitive radio is a different context for communication systems. At the physical layer, it implies that two functions have to be performed by the terminals, namely the assessment of the spectral environment and opportunistic transmission. The physical layer reports to the

upper level decision layers and it receives the instructions for optimal transmission. Filter banks can carry out these two functions efficiently and jointly. The following aspects are worth emphasizing.

- *High performance spectrum sensing.* The filter bank in the receiver is a high performance real time spectrum analyzer. It supplies high quality raw signals to the devices which implement the spectrum sensing strategies.

- *Simultaneous spectrum sensing and transmission.* The same filter bank can be used for sensing and transmission, which ensures performance compatibility. Moreover, thanks to the spectral sub-channel separation, the functions of spectrum analysis and data transmission can be mixed and performed simultaneously. This is a crucial facility for efficient opportunistic communications.

- *Guaranteed spectral protection of neighbouring users.* The out-of-band attenuation curve of the prototype filter sets the level of guaranteed spectral protection of the other users. This is a crucial characteristic for the acceptance of the concept of opportunistic communication.

Finally, FBMC techniques lead to a new physical layer which offers performance gains and additional functionalities in conventional networks and satisfies the criteria for existence and acceptance of new concepts and, particularly, cognitive radio.

**Phydyas website** (<http://www.ict-phydyas.org>)

More details on the techniques presented in this document, as well as alternative and more sophisticated methods, are provided in the following reports, available on the website.

D2.1: Data aided synchronization and initialization for single antenna

D2.2: Blind techniques and strategy

D3.1: Equalization and demodulation in the receiver

D3.2: Optimization of transmitter and receiver

D4.1: MIMO channel matrix estimation and tracking

D4.2: MIMO techniques and beamforming

D5.1: Prototype filter and filter bank structure

D6.1: Duplexing and multiple access techniques

D6.2: Interference and cross-layer

D7.1: Compatibility OFDM/FBMC

D8.1: FBMC in cognitive radio

D8.2: Space-time spectrum sensing

Titles of related conference papers and journal articles are also available on the website.

### ***Annex***

FBMCprimerDemo.m: Matlab demonstration program.